MicroRNA-338-3p regulates age-associated osteoporosis via targeting PCSK5

JIE TONG[1], MIN ZHANG[2], XIA LI[3] and GUOHAI REN[1]

[1]Department of Orthopedics, Affiliated Hospital of Jianghan University, Wuhan, Hubei 430015; [2]Emergency Department, Wuhan Hospital of Traditional Chinese and Western Medicine, Wuhan, Hubei 430022; [3]Department of Ophthalmology and Otorhinolaryngology, Affiliated Hospital of Jianghan University, Wuhan, Hubei 430015, P.R. China

Received June 10, 2020; Accepted October 14, 2020

DOI: 10.3892/mmr.2020.11775

Abstract. Bone loss is a disease that is highly associated with aging. This deleterious health condition has become a public concern worldwide, and there is an urgent need to discover more novel therapeutic strategies for the development of age-associated osteoporosis. The present study aimed to explore the association between proprotein convertase subtilisin/kexin type 5 (PCSK5) and microRNA(miR)-338-3p in bone-formation and bone-loss processes. Western blotting assay and reverse transcription-quantitative PCR were employed to analyze PCSK5 and miR-338-3p expression levels in bone mesenchymal stem cells (BMSCs). Dual-luciferase reporter and RNA pull-down assays were used to determine the target. For osteoblastic differentiation verification, alkaline phosphatase activity, osteocalcin secretion detection, bone formation-related indicators (osterix, runt-related gene 2, osteopontin and bone sialoprotein), hematoxylin and eosin staining and Alizarin Red S staining were performed. The findings of the present study indicated that the expression level of PCSK5 was higher in BMSCs from young rat samples, whereas the expression level of miR-338-3p was higher in BMSCs from samples of old rats. Experimental results also revealed that unlike miR-338-3p, downregulation of PCSK5 inhibited osteoblastic differentiation and osteogenesis by inhibiting alkaline phosphatase, osteocalcin, osterix, runt-related transcription factor 2, osteopontin, bone sialoprotein and mineralized nodule formation. Overall, the results suggested that miR-338-3p could suppress age-associated osteoporosis by regulating PCSK5.

Correspondence to: Dr Guohai Ren, Department of Orthopedics, Affiliated Hospital of Jianghan University, 168 Xianggang Road, Jiangan, Wuhan, Hubei 430015, P.R. China
E-mail: renguohai56@163.com

Key words: proprotein convertase subtilisin/kexin type 5, microRNA-338-3p, osteoporosis, bone mesenchymal stem cells

Introduction

Age-associated osteoporosis can be referred to as a systemic impairment of bone formation and enhancement of bone marrow fat accumulation (1,2). Bone mesenchymal stem cells (BMSCs) can differentiate into osteoblasts or adipocytes and promote bone regeneration (3-5). Tissue regeneration and repair via the differentiation of BMSCs has been a popular topic in regenerative medicine. At the molecular level, the interactions between hormones and transcription factors control mesenchymal stem cell differentiation into osteocytes. The major transcription factors that play a key role in BMSCs differentiation into osteocytes include runt-related transcription factor 2 (RUNX2) and osterix (OSX) (6). Besides, previous studies have used several indicators to detect osteogenic differentiation of BMSCs, such as alkaline phosphatase (ALP), osteocalcin (OCN) secretion, RUNX2, OSX, bone sialoprotein (BSP) and osteopontin (OPN) (7,8).

Although BMSCs gradually lose their capacity to differentiate into osteoblasts, they tend to differentiate into adipocytes in the aging process (9-11). As a result, the ability to form bone declines with age. This association between bone formation and aging is the main cause of the high incidence of age-associated osteoporosis (12,13). Osteoporosis symptoms usually result in fragile bones, thus causing the elderly to experience mobility problems (14). More troubling is that the elderly tend to be more vulnerable to suffer from bone fracture from accidental falls, which increases the financial and emotional burden of family members (15-17). Thus, the treatment of age-associated osteoporosis is of great concern in society. This public health issue has attracted a great deal of attention among medical staff as well as researchers. The purpose of the present study was to gain further insights into the mechanism of bone formation and the occurrence of age-associated osteoporosis using cellular and molecular methods.

Proprotein convertase subtilisin/kexin (PCSK) enzymes are responsible for activating a wide variety of hormones and protein precursors, ranging from growth factors to extracellular pathogens (18). These enzymes cleave and convert their immature target proproteins into an active functional form. One of the important members belonging to this enzyme family is PCSK5, which plays an essential role in a number

of cell activities. As described in a bioinformatics analysis, different Notch signaling components, such as PCSK5, are differential expression factors in osteogenic-differentiation progression (19). In another study, silencing PCSK5 in mice led to severe malformations, bone morphogenic defects and early embryonic lethality, with the absence of growth differentiating factor 11 (20). Based on these previous data, it was speculated that PCSK5 could be a putative therapeutic factor for age-associated osteoporosis. However, no study has comprehensively demonstrated the role of PCSK5, thus the present study was designed to understand how PCSK5 exerts its function in age-associated osteoporosis using BMSCs.

Previous studies have explored the role of miR-338-3p (microRNA-338-3p) in osteoclast formation. A study investigated the expression profile of miR-338-3p in BMSC differentiation, which found that the expression level of miR-338-3p declined as the osteoblast underwent differentiation (21). Thus, miR-338-3p has the potential to participate in the suppression of osteoclast formation and the acceleration of age-associated osteoporosis. Moreover, another study reported that miR-338-3p overexpression in osteoclast precursor cells restricted osteoclast formation (22). Similarly, a study concerning the function of miR-338-3p in osteoclast differentiation and activation demonstrated that miR-338-3p was markedly downregulated during this process (23). In the present study, the mechanism of miR-338-3p in osteoclast formation and the role of the PCSK5 gene in age-associated osteoporosis was explored.

The aim of the present study paper was to study the axis of miR-338-3p targeting PCSK5 in bone formation by exploring their roles in osteoblastic differentiation. The findings of the present study will help to explore some novel therapeutic methods for age-associated osteoporosis.

Materials and methods

Bioinformatics analysis. The GEO profile (GSE35959) (24) was downloaded from the National Center for Biotechnology Information (https://www.ncbi.nlm.nih.gov/). The dataset was used to screen the downregulated differentially expressed genes (DEGs) with $P<0.05$ and $\log_2$-fold-change ($\log_2$FC) <-2. Metascape (http://metascape.org/gp/index.html#/main/step1) was subsequently used to enrich the biological processes of the top 100 downregulated DEGs. Next, TargetScan Human v7.1 (http://www.targetscan.org/vert_71/), starBase v2.0 (http://starbase.sysu.edu.cn/index.php) and miRDB (http://mirdb.org/) were applied to predict the miRNAs that bind to the PCSK5 3' untranslated region (UTR). The overlapping miRNAs were identified using Venny 2.1 (https://bioinfogp.cnb.csic.es/tools/venny/).

Hematoxylin and eosin staining (H&E). H&E staining was employed to detect the morphology of the distal tibia in rats. A total of 18 male rats, six in each group, were divided into young group (3 months; 260±10 g), middle-aged group (12 months; 360±10 g) and old group (18 months; 450±10 g). The Sprague-Dawley rats were purchased from Nanjing Junke Bioengineering (Jiangsu, China). Rats were kept on a 12-h light/dark cycle at 20-25˚C with 60% relative humidity under specific pathogen-free conditions, and fed a non-purified diet with free access to water ad libitum. All animal procedures were approved by the Animal Ethics Committee of Affiliated Hospital of Jianghan University (approval no. JH-20191014-23; Jiangan, China).

Rats were euthanized by CO_2 asphyxiation (fill rate of 20% of the chamber volume/min with CO_2), and the tibia was harvested after the rats had no vital signs, such as lack of breath and faded eye color. The tibia of the rats was subsequently fixed in 10% formalin solution for 2 days at room temperature and decalcified slowly with EDTA. Next, the tissue was dehydrated at room temperature in gradient concentrations of ethanol (70, 80, 90, 95 and 100%) every 2-5 min, embedded in paraffin and then sliced to 5-μm thick sections. The tissue sections were subsequently stained with hematoxylin for 5 min and treated with 1% hydrochloric acid ethanol solution for 5 sec at room temperature. After that, a 1% ammonia solution was used to reverse the blue, 1% eosin solution was used to stain the cytoplasm for 3 min, and the sections were finally dehydrated until translucent at room temperature. Finally, the images were sealed with neutral resin and analyzed with IPP6.0 image analysis software (Media Cybernetics, Inc.).

Cell culture and differentiation. BMSCs were obtained from the femur and tibia of rats at the age of 3 (young), 12 (middle-aged) and 18- (old-aged) months. The procedure was carried out as follows: i) firstly, the medullary cavity was thoroughly flushed the using an α-modified Eagle's medium (αMEM; Invitrogen; Thermo Fisher Scientific, Inc.) without ascorbic acid to collect the cells. The cells were then allowed attach in complete αMEM with 10% FBS, 1% penicillin and streptomycin (all from Gibco; Thermo Fisher Scientific, Inc.) at 37˚C, 5% CO_2 for 72 h. Following this step, BMSCs were finally obtained by replacing the fresh culture medium. For the induction of osteogenic differentiation, BMSCs were cultured for 16 days in osteogenesis induction αMEM medium with 10% FBS, 300 ng/ml bone morphogenetic protein 2 (Gibco; Thermo Fisher Scientific, Inc.), 50 μg/ml ascorbic acid (Gibco; Thermo Fisher Scientific, Inc.) and 5 mM β-glycerolphosphate (Gibco; Thermo Fisher Scientific, Inc.).

Cell transfection. Small interference (si)RNA si-PCSK5, miR-338-3p mimic, miR-338-3p inhibitor and their non-targeting sequence negative controls (NC) were designed by Genewiz, Inc. The corresponding sequences are listed in Table SI. The transfection was performed in middle-aged rat-derived BMSCs at the point of ~70% cell confluence using Lipofectamine® 3000 reagent (Invitrogen; Thermo Fisher Scientific, Inc.), according to the manufacturer's instructions. The densities of BMSCs seeded into 6-, 12-, 24- and 96-well plates were $2.5x10^6$, $1x10^6$, $5x10^5$ and $5x10^4$ cells per ml, respectively. The transfection concentration of si-PCSK5 was 2.5 μM, while that of miR-338-3p mimic, miR-338-3p inhibitor and negative control was 50 nM. The untransfected BMSCs were set as the CON group. After transfection for 48 h, the transfection efficiency was detected using reverse transcription-quantitative (RT-q)PCR and the follow-up experiments were carried out.

RNA isolation, cDNA synthesis and RT-qPCR. A complete RNA isolation was performed using the Cell Total RNA

Isolation kit (ForeGene). Using RT Easy™ II (Fore Gene), according to the manufacturer's protocol, cDNA synthesis was performed. Following which, mRNA expression and miRNA expression levels were measured by RT-qPCR using the Bio-Rad CFX96 Touch system (Bio-Rad Laboratories, Inc.) and iTaq™ Universal SYBR GREEN Supermix (Bio-Rad Laboratories, Inc.). The RT-qPCR thermocycling conditions were: 50˚C for 2 min, at 95˚C for 30 sec, and then 40 cycles of 15 sec at 95˚C and 30 sec at 60˚C. Two reference genes U6 and GAPDH were used to quantify miRNA and mRNA, respectively. To calculate mRNA expression, the $2^{-\Delta\Delta Cq}$ (25) method was employed. The sequences of primers are listed in Table I.

Western blotting. For the collection of protein samples, the cells were washed with cold PBS. The cells were then lysed with radio immunoprecipitation assay lysis buffer (Roche Diagnostics GmBH) containing 10 mM Tris, pH 7.5, 150 mM NaCl, 0.1% SDS, 1.0% Triton X-100, 1% deoxycholate, 5 mM EDTA, 1 mM sodium orthovanadate, 1 mM phenylmethylsulfonyl fluoride and protease inhibitor cocktail on ice for 15 min. The cells were then transferred into pre-cooled 1.5 ml centrifuge tubes. After obtaining the supernatant (protein samples), their concentrations were measured using a BCA Protein Assay Reagent kit (Pierce; Thermo Fisher Scientific, Inc.) Next, 30 μg protein sample was added into the wells of an 8% SDS-PAGE gel for electrophoresis at 80 V for 20 min and later 100 V for 1 h. The PVDF membrane was subsequently used in the present experiment, and the transfer current was set at 200 mA. Following this step, the protein membrane was added to the prepared PBS solution and rinsed twice. The PBS solution, which contained 5% skimmed milk powder, was then added for a 60-min blocking at room temperature. After washing with PBS, anti-PCSK5 (1:500; cat. no. 16470-1-AP) and β-actin (1:1,000; cat. no. 20536-1-AP) (both from Proteintech Group, Inc.) were added and incubated overnight at 4˚C. HRP-conjugated Affinipure goat anti-rabbit IgG (H+L) (1:5,000; cat. no. SA00001-2; Proteintech, Group, Inc.) was added to the membrane for incubation at room temperature for 1 h. After the secondary antibody incubation, the product was washed three times with PBS. The immunoreactive bands were visualized using the ECL-PLUS kit (Cytiva) according to the manufacturer's manual. The results and the images were analyzed with the Gel image analysis system and the Gel-Pro Analyzer 3.1 (Media Cybernetics, Inc.), respectively. The gray value of the bands was analyzed by Image J2x software (Rawak Software Inc.). In this procedure, β-actin was used as the reference gene.

ALP activity and osteocalcin secretion detection. BMSCs ($1x10^5$ cells/well) were seeded onto a 24-well plate with an osteogenesis induction αMEM for 48 h. Using the colorimetric ALP Activity Assay kit (Abcam), the cells were subjected to lysis to detect ALP activity. More specifically, BMSCs were harvested, washed with cold PBS, resuspended in 50 μl Assay Buffer, and then homogenized with a Dounce homogenizer (Thermo Fisher Scientific, Inc.) on ice. Subsequently, the samples were centrifuged at 4˚C at 13,000 x g for 15 min in a cold microcentrifuge. This step was performed to remove any insoluble materials. Following that, the supernatant was collected and transferred into a new tube. Next, 20 μl STOP Solution was added to sample background control wells to terminate ALP activity in these samples. Next, 50 μl pNPP solution (5 mM) was added to each well containing sample and background sample controls. After that, 10 μl ALP enzyme solution was added to each pNPP standard well for an incubation period of 60 min at 25˚C in the dark. The reaction was halted by adding 20 μl STOP Solution. The optical absorbance was finally measured at 450 nm using a microplate reader (Thermo Fisher Scientific, Inc.).

Table I. Primer sequences for reverse transcription-quantitative PCR.

Gene	Primer sequences (5'→3')
miR-338-3p	Forward: TCCAGCATCAGTGATTTTGTTG
	Reverse: GTGCAGGGTCCGAGGT
U6	Forward: GCTTCGGCAGCACATATA
	Reverse: CGCTTCACGAATTTGCGT
PCSK5	Forward: CAACACACATCCTTGCCAGTC
	Reverse: ATGTTCTTCCCCGTGTAGCC
OSX	Forward: CCTCCTCAGCTCACCTTCTC
	Reverse: GTTGGGAGCCCAAATAGAAA
RUNX2	Forward: GACCAGTCTTACCCCTCCTACC
	Reverse: CTGCCTGGCTCTTCTTACTGAG
OPN	Forward: CAGTTGTCCCCACAGTAGACAC
	Reverse: GTGATGTCCTCGTCTGTAGCATC
BSP	Forward: GAATGGCCTGTGCTTTCTCAA
	Reverse: TCGGATGAGTCACTACTGCCC
GAPDH	Forward: GCTGGTCATCAACGGGAAA
	Reverse: CGCCAGTAGACTCCACGACAT

miR-338-3p, microRNA-338-3p; PCSK5, proprotein convertase subtilisin/kexin type 5; OSX, osterix; RUNX2, Runt-related gene 2; OPN, osteopontin; BSP, bone sialoprotein.

In order to detect osteocalcin secretion, BMSCs (treated with 0.25% trypsin) were first mixed with PBS and then transferred into single-cell suspension repeatedly. The cells were later crushed completely by repeated freeze-thaw at -20˚C. After ensuring cell suspension was centrifuged for 20 min at 1,667 x g and 4˚C, the supernatant was collected. The osteocalcin secretion was later detected with the Osteocalcin ELISA Detection kit (cat. no. AC-11F1; Immunodiagnostic Systems, Ltd.).

Alizarin Red S staining. Alizarin Red S staining was performed to evaluate mineralization deposition in BMSCs, which had been cultured in a 6-well plate with osteogenesis induction medium for 21 days. The cells were incubated with 1 ml 10% formaldehyde for 10 min at room temperature. After which, the cells were washed twice with PBS. Then, 1 ml 2% Alizarin Red S solution (pH was adjusted to ~4.5 with 0.5% ammonium hydroxide) was added to the cells for 15 min cellular staining at 25˚C. Following the staining, the stained cells were thoroughly washed with double-distilled water (ddH_2O). The stained cells in each well were subsequently

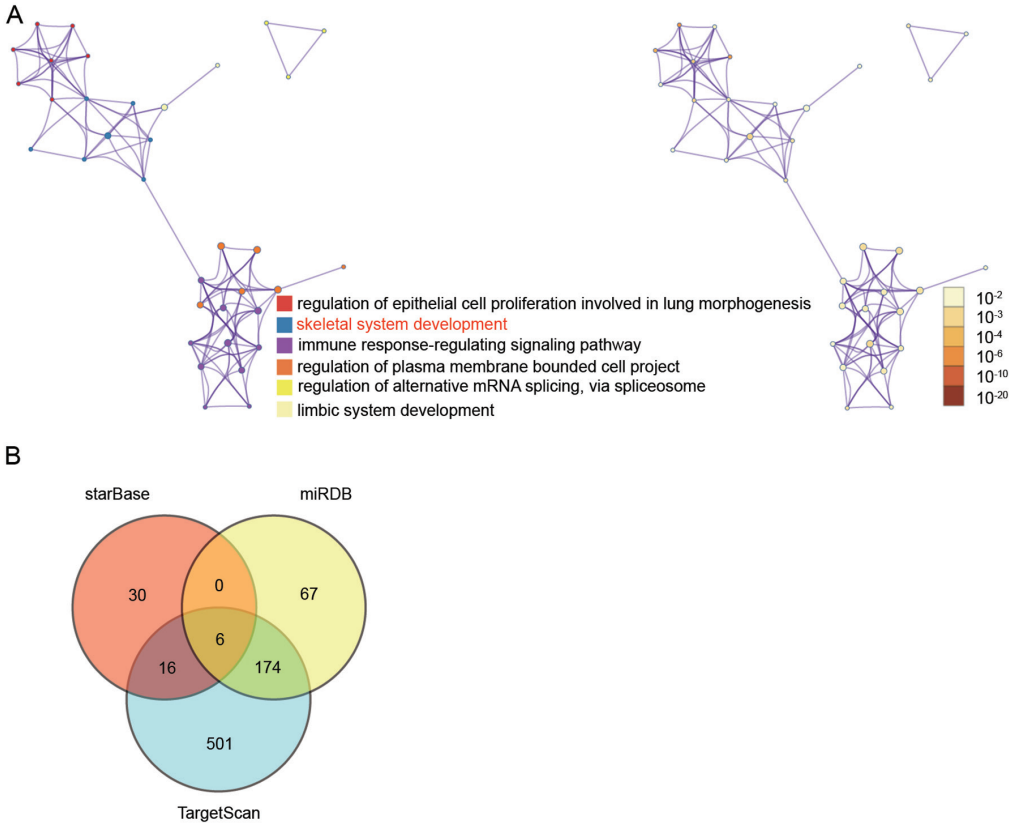

Figure 1. Screening of key genes and miRNAs associated with the effect of age on BMSCs. (A) Skeletal system development was demonstrated by Metascape analysis to be the key biological process involving eight genes. Metascape was the online tool that was used for the enrichment of top 100 downregulated differentially expressed genes from GSE35959. (B) TargetScan, starBase, and miRDB were the databases that were used to predict miRNAs binding to proprotein convertase subtilisin/kexin type 5; a total of six miRNAs were overlapped. miRNA, microRNA; BMSCs, bone mesenchymal stem cells.

captured by an optical microscope (Olympus Corporation) at x200 magnification. Following which, the positively stained area (red) was observed in Image Pro Plus 6.0 (Media Cybernetics, Inc.).

Dual-luciferase reporter assay. The binding site of miR-338-3p to PCSK5 3'UTR was 'AUGCUGG', which was also the sequence of PCSK5 wild type (PCSK5 WT). To generate PCSK5 mutant type (PCSK5 MUT), 'AUGCUGG' was replaced by 'UACGACC'. Next, the pmiR-GLO reporter vector with PCSK5 WT (100 ng) or MUT (100 ng) was co-transfected with miR-338-3p mimic (50 nM) or mimic NC (50 nM) using Lipofectamine 3000 reagent. The pmiR-GLO reporter vector, miR-338-3p mimic and mimic NC were all purchased from Promega Corporation. BMSCs were subsequently seeded in a 96-well plate for an incubation period of 48 h after the co-transfection. The relative luciferase activity, which could be a strong reference for the association between miR-338-3p and its target gene PCSK5, was measured using a dual-luciferase reporter assay system (Promega Corporation). Renilla luciferase acted as an internal control to normalize the luciferase activity.

RNA pull-down. The pull-down assay with biotinylated miRNA was performed according to the methodology used in a previous study (26). BMSCs were seeded into a 6-well plate. Following which, 100 nM biotinylated miR-338-3p mimic (Bio-miR-338-3p) or biotinylated negative control (Bio-NC) (Guangzhou RiboBio Co., Ltd.) was transfected into BMSCs. After the 48-h transfection, the cells were washed with PBS and then lysed using a specific lysis buffer containing 20 mM Tris, pH 7.5, 200 mM NaCl, 2.5 mM $MgCl_2$, 0.05% Igepal, 60 U/ml Superase-In (cat. no. AM2694; Invitrogen; Thermo Fisher Scientific, Inc.), 1 mM DTT (cat. no. 3483-12-3; EMD Millipore), and protease inhibitors. Streptavidin magnetic beads 100 μl (Invitrogen; Thermo Fisher Scientific, Inc.) were subsequently used to pull down the biotin-coupled RNA complex after incubating the samples for 4 h. Next, the beads were attracted by a magnetic grate (Invitrogen; Thermo Fisher Scientific, Inc.). The abundance of PCSK5 was eventually evaluated using RT-qPCR.

Statistical analysis. Three independent experiments were performed, and quantitative data were presented as the mean ± standard deviation (SD). Statistical significance was determined by employing Student's unpaired t-tests or one-way ANOVA with Dunnett's multiple comparisons test or Tukey's multiple comparisons test. $P<0.05$ was considered to indicate a statistically significant difference.

Results

PCSK5 and miR-338-3p are key regulators of BMSCs. The 222 downregulated DEGs were first screened out from GSE35959 with $P<0.05$ and $\log_2FC$ <-2. The top 100 downregulated DEGs were subsequently uploaded to Metascape

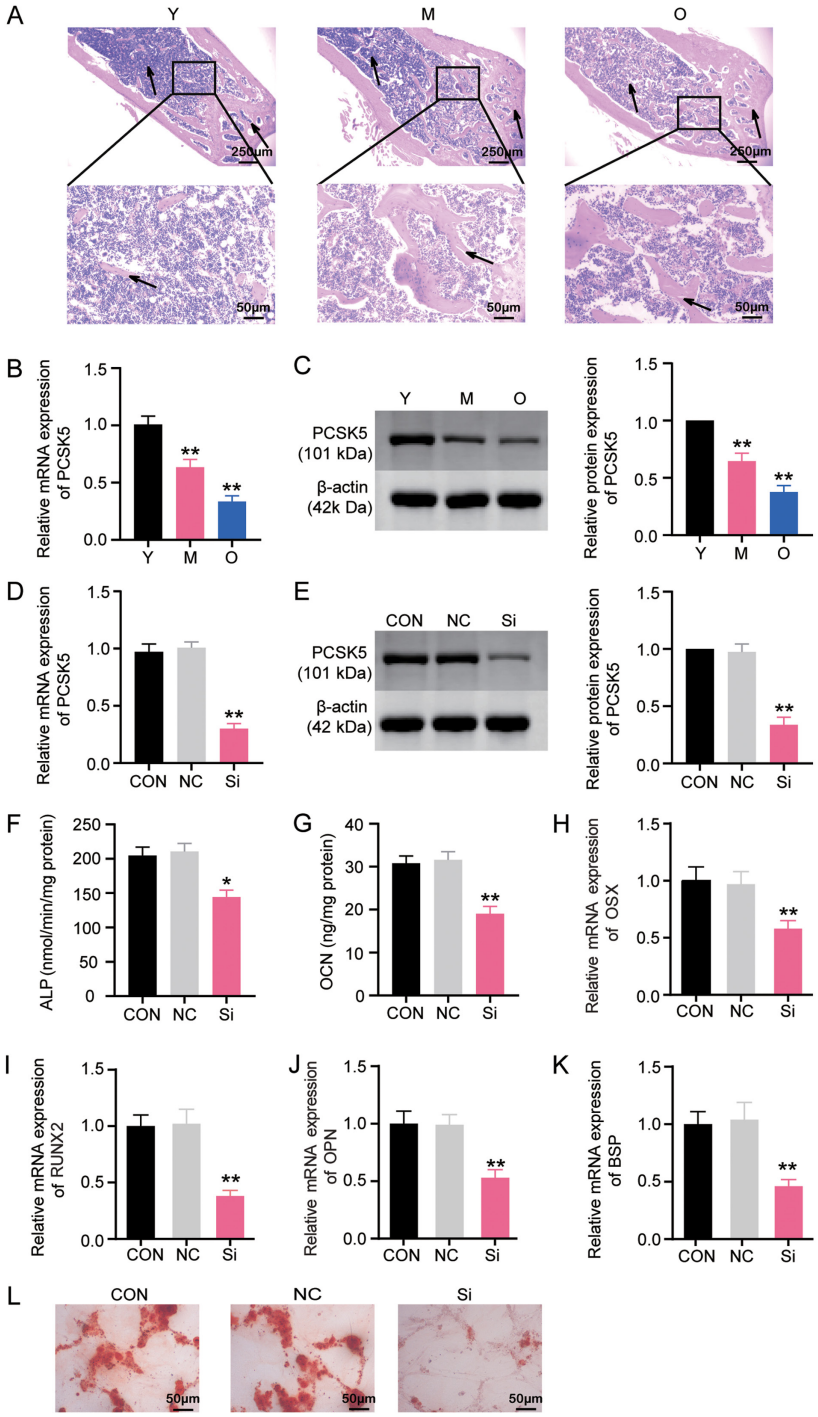

Figure 2. PCSK5 contributes to osteoblastic differentiation of BMSCs. (A) Representative images of the proximal tibial metaphysis from rats of the Y, M and O groups detected by staining with hematoxylin and eosin. Magnifications, x40 and x200. n=6. (B) Expression of PCSK5 mRNA in BMSCs from rats in Y, M and O groups using RT-qPCR. n=6. (C) Expression of PCSK5 protein in BMSCs of rats in Y, M and O groups using western blot assay. n=6. (D) Inhibitory efficiency of si-PCSK5 in BMSCs by RT-qPCR. (E) Inhibitory efficiency of si-PCSK5 in BMSCs using western blot analysis. (F) Analysis of ALP activity after the transfection of si-PCSK5 or NC into BMSCs induced for osteoblastic differentiation for 48 h. (G) OCN secretion detection after the transfection of si-PCSK5 or NC into BMSCs induced for differentiation for 48 h. mRNA expression detection of (H) OSX, (I) RUNX2, (J) OPN and (K) BSP after the transfection of si-PCSK5 or NC into BMSCs induced for differentiation for 48 h. (L) Representative images of Alizarin Red S staining of BMSCs after osteoblastic differentiation for 21 days. Magnification, x200. Data are presented as the mean ± SD. Statistical significance was determined using one-way ANOVA. n=3. *P<0.05 and **P<0.001 vs. control group. BMSCs, bone mesenchymal stem cells; PCSK5, proprotein convertase subtilisin/kexin type 5; Y, 3-month-old young rats; M, 12-month-old middle-aged rats; O, 18-month-old aged rats; OPN, osteopontin; RT-qPCR:, reverse transcription-quantitative PCR; si-PCSK5, small interfering RNA targeting PCSK5; NC, negative control siRNA; ALP, alkaline phosphatase; OCN, osteocalcin secretion; OSX, osterix; RUNX2, runt-related gene 2; OPN, osteopontin; BSP, bone sialoprotein; CON, normal control.

for enrichment analysis. As shown in Fig. 1A, the skeletal system development was identified as the key biological process involving eight genes: FGFR2, NFIB, PCSK5, RPL38, SFRP2, COL14A1, WASF2 and ANKRD11. In one study, PCSK5 was reported to be responsible for bone development (27). Besides, mice lacking PCSK5 exhibit bone

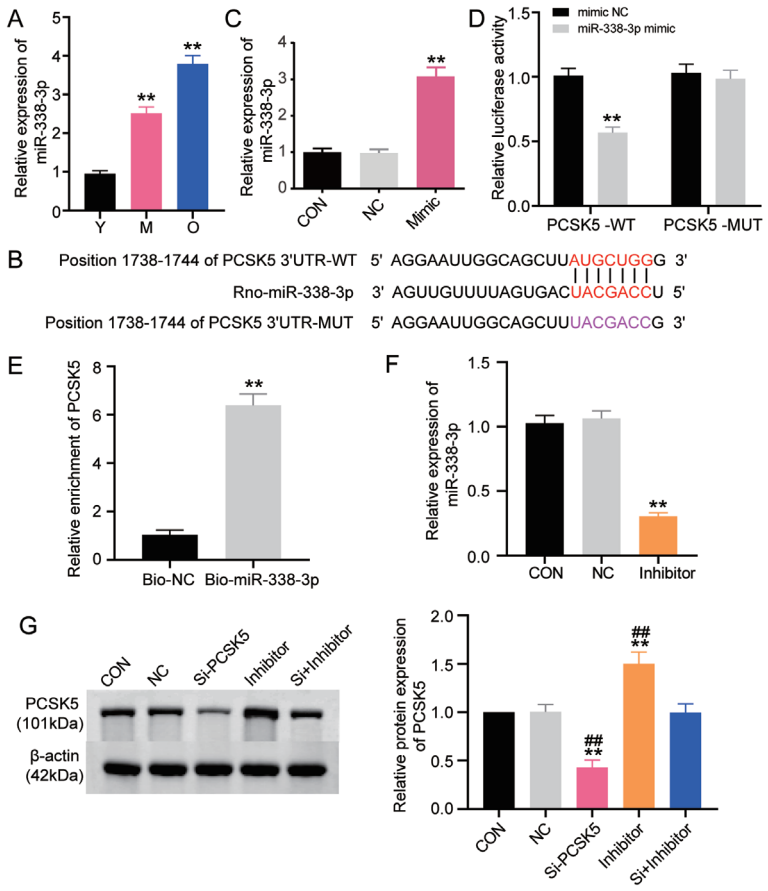

Figure 3. PCSK5 is a target of miR-338-3p. (A) Expression of miR-338-3p in BMSCs from rats in groups Y, M and O by RT-qPCR. (B) PCSK5-WT or PCSK5-MUT without or with the binding sequence of miR-338-3p. (C) Transfection efficiency of miR-338-3p mimic in BMSCs was detected by RT-qPCR. (D) The association between miR-338-3p and PCSK5 was detected using dual-luciferase reporter assay. (E) The target association of miR-338-3p with PCSK5 was detected with RNA pull-down assay system. (F) Inhibitory efficiency of miR-338-3p inhibitor in BMSCs by RT-qPCR. (G) Expression of PCSK5 protein was measured using western blotting when miR-338-3p was silenced by the miR-338-3p inhibitor. Data are presented as the mean ± SD. Statistical significance was determined with unpaired Student's t-test or one-way ANOVA. n=3. **P<0.001 vs. control group; $^{\#\#}$P<0.001 vs. si+inhibitor group. PCSK5, proprotein convertase subtilisin/kexin type 5; miR, microRNA; RT-qPCR, reverse transcription-quantitative PCR; Y, 3-month-old young rats; M, 12-month-old middle-aged rats; O, 18-month-old aged rats; BMSCs, bone mesenchymal stem cells; Bio-NC, biotinylated negative control; bio-miR-338-3p, biotinylated miR-338-3p mimic; CON, normal control; NC, negative control; si-PCSK5, small interfering RNA targeting PCSK5; inhibitor, miR-338-3p inhibitor; UTR, untranslated region; WT, wild-type; MUT, mutant.

morphogenic defects (20). PCSK5 was, therefore, identified as the gene of interest to be investigated in the present study. To identify the key miRNAs that could target PCSK5, starBase, miRDB and TargetScan were applied. Finally, six overlapping miRNAs were found by Venny 2.1.0 (Fig. 1B); they included hsa-miR-29a-3p, hsa-miR-29b-3p, hsa-miR-29c-3p, hsa-miR-338-3p, hsa-miR-577 and hsa-miR-664b-3p. Based on a previous study, miR-338-3p required further investigation due to its downregulation during osteoblast differentiation (21).

PCSK5 contributes to osteoblastic differentiation of BMSCs. H&E staining was first used to examine the morphology of the proximal tibial of 3-month-old young rats (Y), 12-month-old middle-aged rats (M) and 18-month-old aged rats (O). Findings revealed that with aging, obvious bone defects existed in the metaphysis of the proximal tibial. More specifically, the osteoid content decreased, and the fracture and separation of the trabecular meshwork appeared (Fig. 2A). Next, mRNA and protein expression of PCSK5 in BMSCs harvested from rats of different age stages was measured, including 3-month-old young rats (Y), 12-month-old middle-aged rats (M) and 18-month-old aged rats (O). It was observed that both mRNA and protein expression of PCSK5 declined as the age of the rats increased (Fig. 2B and C). More specifically, the mRNA expression of PCSK5 in the M group was 60% of the Y group, while the O group was only 30% of the Y group (Fig. 2B). The protein expression of PCSK5 in the M group was 70% of the Y group, whereas the O group was only 40% of the Y group (Fig. 2C). To obtain an improved understanding of the role of PCSK5 in age-associated osteoporosis progression, si-PCSK5 was synthesized to knock down PCSK5, and was transfected into BMSCs derived from middle-aged rats. The results of RT-qPCR showed that si-PCSK5 could notably decrease the mRNA expression of PCSK5 by ~70% compared with the control group (Fig. 2D). Western blotting results also showed that the protein expression of PCSK5 was reduced by si-PCSK5 by ~65% compared with the control group (Fig. 2E). These results demonstrated that si-PCSK5 could successfully decrease the expression of PCSK5 at both mRNA and protein levels. Therefore, si-PCSK5 was employed in the subsequent experiments.

To comprehensively unravel the role of PCSK5 in osteoblastic differentiation, si-PCSK5 or its NC was transfected

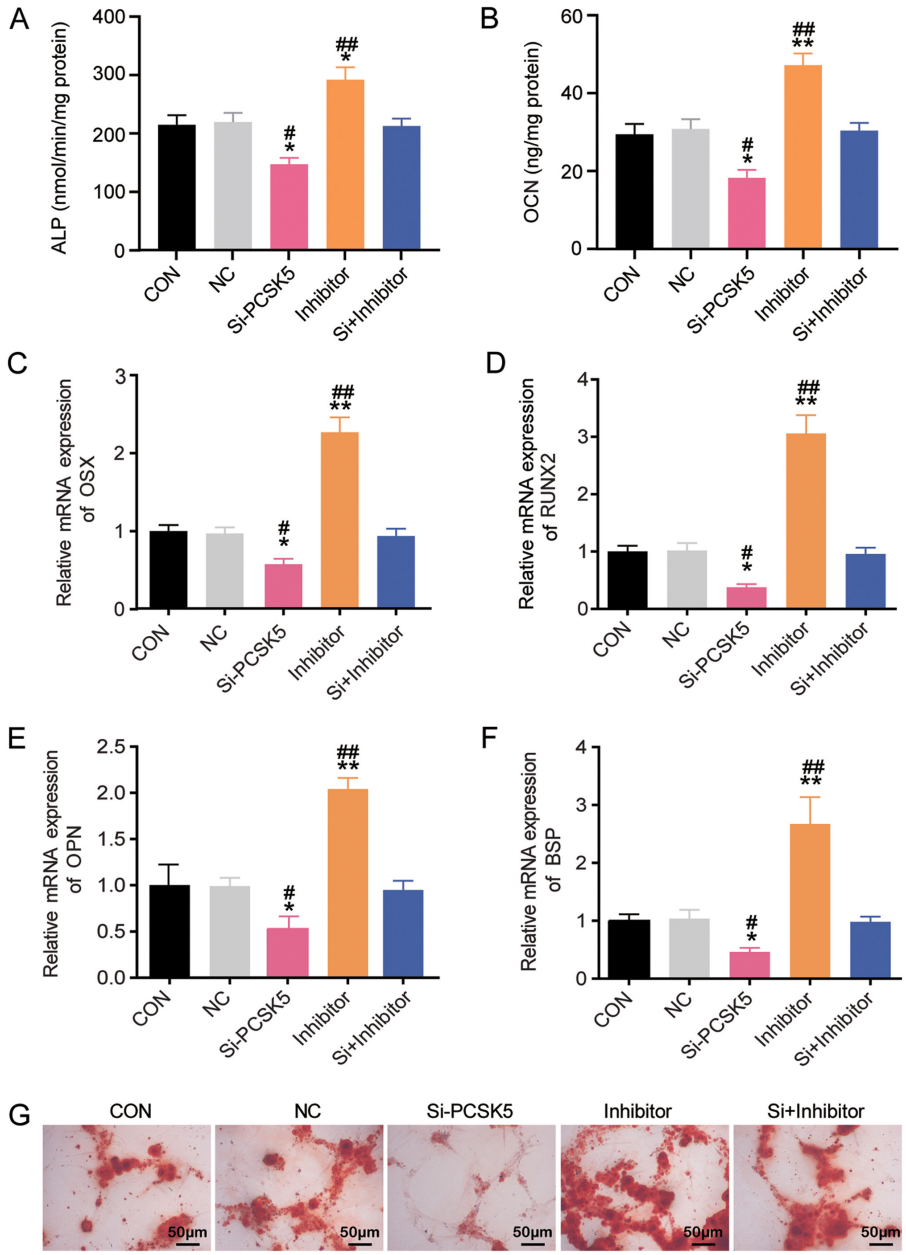

Figure 4. miR-338-3p inhibits osteoblastic differentiation of BMSCs by targeting PCSK5. (A) ALP activity was evaluated after the transfection of si-PCSK5, miR-338-3p inhibitor or si-PCSK5 plus miR-338-3p inhibitor in BMSCs. (B) OCN secretion was detected after transfection with si-PCSK5, miR-338-3p inhibitor or si-PCSK5 plus miR-338-3p inhibitor in BMSCs. (C) OSX mRNA expression was measured after transfection with si-PCSK5, miR-338-3p inhibitor or si-PCSK5 plus miR-338-3p inhibitor in BMSCs. (D) RUNX2 mRNA expression was evaluated after transfection with si-PCSK5, miR-338-3p inhibitor or si-PCSK5 plus miR-338-3p inhibitor in BMSCs. (E) OPN mRNA expression was measured after transfection with si-PCSK5, miR-338-3p inhibitor or si-PCSK5 plus miR-338-3p inhibitor in BMSCs. (F) BSP mRNA expression was measured after transfection with si-PCSK5, miR-338-3p inhibitor or si-PCSK5 plus miR-338-3p inhibitor in BMSCs. (G) Alizarin Red S staining was measured after transfection with si-PCSK5, miR-338-3p inhibitor or si-PCSK5 plus miR-338-3p inhibitor in BMSCs. Magnification, x200. Data are presented as the mean ± SD. Statistical significance was determined using one-way ANOVA. n=3. *P<0.05 and **P<0.001 vs. control group; $^{\#}$P<0.05 and $^{\#\#}$P<0.001 vs. si+inhibitor group. PCSK5, proprotein convertase subtilisin/kexin type 5; BMSCs, bone mesenchymal stem cells; miR, microRNA; OSX, osterix; ALP, alkaline phosphatase; OCN, osteocalcin; OSX, osterix; RUNX2, Runt-related gene 2; OPN, osteopontin; BSP, bone sialoprotein; CON, normal control; NC, negative control; inhibitor, miR-338-3p inhibitor; si-PCSK5, small interfering RNA targeting PCSK5.

into BMSCs for 48 h, which were induced to differentiate into osteoblasts. Since OCN, ALP, OSX, RUNX2, OPN and BSP are popular markers for osteoblastic differentiation, these markers were detected to investigate the process of osteoblastic differentiation. After testing for ALP activity and osteocalcin secretion, it was found that si-PCSK5 restrained ALP activity by 30% compared with the control group (Fig. 2F) and that it suppressed osteocalcin secretion by ~35% compared with the control group (Fig. 2G). The mRNA expression levels of OSX, RUNX2, OPN and BSP (Fig. 2H-K) were also examined. The findings indicated that the mRNA expression levels of OSX and OPN decreased by ~40%, whereas the mRNA expression levels of RUNX2 and BSP decreased by ~60% (Fig. 2H-K). Furthermore, Alizarin Red S staining was performed after a 21-day induction of osteoblastic differentiation. The images showed that si-PCSK5 suppressed mineralized nodule

formation in BMSCs (Fig. 2L). Taken together, the results demonstrated that PCSK5 contributes to the osteoblastic differentiation of BMSCs.

PCSK5 is a target of miR-338-3p. To explore the mechanism of PCSK5 in the regulation of age-associated osteoporosis, the targets upstream of PCSK5 were investigated. The literature has established that a number of genes are mediated by various miRNAs. Hence, TargetScan was used to predict the potential miRNAs that could bind to PCSK5 3'UTR. Venny 2.1 analyses revealed that miR-338-3p could target PCSK5 (Fig. 1B). To confirm this, RT-qPCR was used to examine the mRNA expression of miR-338-3p in BMSCs from the Y, M and O groups of rats. The results showed that the expression of miR-338-3p in the M group was upregulated 2.5 times as much as the Y group (Fig. 3A). However, the expression of miR-338-3p in the O group was found to be significantly upregulated 4 times as much as the Y group. This outcome was completely opposite to that of PCSK5 (Fig. 3A). Next, a dual-luciferase reporter assay kit was utilized to verify whether PCSK5 was the exact target gene of miR-338-3p. The wild-type (PCSK5-WT) and mutant type (PCSK5-MUT) of PCSK5 were first generated (Fig. 3B) and then co-transfected with miR-338-3p mimic or mimic NC into BMSCs. Following transfection with miR-338-3p mimic, RT-qPCR demonstrated that the expression level of miR-338-3p increased by ~3 times compared with the mimic NC group (Fig. 3C). Following co-transfection, as illustrated in Fig. 3D, the group of PCSK5-WT plus miR-338-3p mimic suppressed luciferase activity by 40% compared with the group of PCSK5-WT plus mimic NC. Luciferase activity was not influenced in the mutant group, meaning miR-338-3p could bind to PCSK5 3'UTR; this was further confirmed by the RNA pull-down assay. As depicted in Fig. 3E, the expression of PCSK5 was dramatically enriched in the Bio-miR-338-3p group by >6 times compared with the Bio-NC group. This result suggested that miR-338-3p could target PCSK5. Subsequently, miR-338-3p inhibitor was applied to silence miR-338-3p. The inhibitory efficiency detected using RT-qPCR showed that miR-338-3p inhibitor successfully decreased the expression of miR-338-3p to a level that was 30% of the control group (Fig. 3F). The expression of PCSK5 protein was detected by western blotting, following transfection with si-PCSK5, miR-338-3p inhibitor or si-PCSK5 plus miR-338-3p inhibitor in BMSCs. The results indicated that the expression of PCSK5 protein was suppressed by si-PCSK5 by 60%, while it was enhanced by the miR-338-3p inhibitor by 50% compared with the control group (Fig. 3G). The expression of PCSK5 protein, which was suppressed by si-PCSK5, could even be reversed by the miR-338-3p inhibitor. These results revealed that the expression of PCSK5 protein could be increased if miR-338-3p was silenced. Given that miR-338-3p could suppress PCSK5 on the protein level, miR-338-3p could target PCSK5.

miR-338-3p inhibits osteoblastic differentiation of BMSCs. Given that PCSK5 is a potential target of miR-338-3p, whether or not miR-338-3p exerted the opposite effect to PCSK5 on osteoblastic differentiation of BMSCs was verified. To confirm this, BMSCs were transfected with si-PCSK5, miR-338-3p inhibitor, si-PCSK5 plus miR-338-3p inhibitor, and NC. Similar to the exploration of PCSK5, ALP activity, OCN secretion, OSX, RUNX2, OPN and BSP mRNA expression and Alizarin Red S staining were conducted in BMSCs. As shown in Fig. 4A, the miR-338-3p inhibitor increased ALP activity by 40% compared to the control group, and it compromised the inhibitory effect of si-PCSK5 on ALP activity. Compared with the control group, the secretion of OCN was enhanced by 60% when miR-338-3p was inhibited (Fig. 4B). Also, the braking effect of si-PCSK5 on osteocalcin secretion was restored by the miR-338-3p inhibitor (Fig. 4B). Compared with the control group, miR-338-3p inhibitor increased the mRNA expression of OSX, RUNX2, OPN and BSP by ~2.3, 3, 2 and 2.5 times, and it weakened the inhibition of si-PCSK5 on OSX, RUNX2, BSP and OPN mRNA expression (Fig. 4C-F). Alizarin Red S staining showed that mineralized nodule formation was facilitated in BMSCs with the miR-338-3p inhibitor (Fig. 4G) and that the miR-338-3p inhibitor could reverse the effect of si-PCSK5. Overall, these results demonstrated that miR-338-3p inhibited osteoblastic differentiation of BMSCs, thereby playing an opposite role of PCSK5 in age-associated osteoporosis.

Discussion

In the present study, the regulatory mechanism of miR-338-3p and its target gene PCSK5 on osteogenic differentiation was investigated *in vitro* using BMSCs. The aim was to gain more insights into the effects of miR-338-3p and its target gene PCSK5 on the osteogenesis process, as well as understanding their roles in age-associated osteoporosis. The experimental results showed that miR-338-3p inhibited osteogenic differentiation, while its target gene PCSK5 accelerated osteogenic differentiation. Therefore, miR-338-3p may be a potential regulator that inhibits osteogenesis and promotes age-associated osteoporosis, even though its target gene PCSK5 had the opposite effect. A previous study reported that PCSK5 was localized in bone tissues and expressed in osteoblasts and osteocytes (28). The detection of mRNA and protein expression of PCSK5 in BMSCs in the present study at different stages of the aging process confirmed that PCSK5 had an inverse relationship with age. Thus, PCSK5 was suspected to be involved in the regulation of bone formation. A previous study suggested that PCSK5 was a putative regulator in skeletal development (27). Similarly, the present identified PCSK5 as an essential regulatory factor in bone formation by contributing to osteoblastic differentiation. As osteogenesis is a process that highly involves osteoblastic differentiation (29), the promotional effect of PCSK5 on osteoblastic differentiation reflected its positive role in osteogenesis. Bone deterioration is even caused by a decrease in osteogenesis function (30). Based on this, it is proposed that PCSK5 is crucial in protecting against age-associated osteoporosis.

In addition, the role of miR-338-3p in osteoblastic differentiation was illustrated in the present study. To be more specific, it was verified that miR-338-3p could target PCSK5. The findings revealed that miR-338-3p showed an opposite trend of expression in BMSCs with age and exerted negative functions on PCSK5, thereby limiting bone formation. Several studies also reported that an increasing number of miRNAs could regulate BMSC differentiation (31-33). In the present study, increased expression of miR-338-3p was observed in BMSCs of older rat samples, which indicated a counter-productive role of miR-338-3p in osteogenesis. Furthermore, it was demonstrated

that the enrichment of miR-338-3p resulted in the reduction of osteoblastic differentiation in BMSCs. The present results were consistent with an *in vitro* analysis that showed that miR-338-3p inhibited the expression of osteoblastic differentiation markers, such as OSX, which suppressed osteoblastic differentiation (21). Playing an inhibitory role in osteoblastic differentiation, miR-338-3p could also be an inducer of bone loss and age-associated osteoporosis.

According to previous studies, several factors contribute to promote bone formation and suppress bone resorption (34-36). In the present study, experiments were not designed that were relevant to investigate the crosstalk among miR-338-3p or PCSK5. Future research may focus on this process and explain the underlying mechanism of miR-338-3p or PCSK5 in osteogenesis as well as age-associated osteoporosis.

In summary, the experiments carried out in the present study demonstrated that PCSK5 targeted by miR-338-3p could restrict the process of age-associated osteoporosis by contributing to osteogenesis. Thus, PCSK5 and its upstream target miR-338-3p could be valuable biomarkers for the prevention and healing of age-associated osteoporosis.

Acknowledgements

Not applicable.

Funding

No funding was received.

Availability of data and materials

The datasets used and/or analyzed during the current study are available from the corresponding author on reasonable request.

Authors' contributions

JT conceived and designed the study. MZ acquired the data. XL performed the data analysis. GR interpreted the data. All authors read and approved the final manuscript.

Ethics approval and consent to participate

All animal procedures were approved by the Animal Ethics Committee of Affiliated Hospital of Jianghan University (approval no. JH-20191014-23; Jiangan, China).

Patient consent for publication

Not applicable.

Competing interests

The authors declare that they have no competing interests.

References

1. Kiernan J, Hu S, Grynpas MD, Davies JE and Stanford WL: Systemic Mesenchymal Stromal Cell Transplantation Prevents Functional Bone Loss in a Mouse Model of Age-Related Osteoporosis. Stem Cells Transl Med 5: 683-693, 2016.
2. Compston JE, McClung MR and Leslie WD: Osteoporosis. Lancet 393: 364-376, 2019.
3. Prockop DJ: Marrow stromal cells as stem cells for nonhematopoietic tissues. Science 276: 71-74, 1997.
4. Chen Q, Shou P, Zheng C, Jiang M, Cao G, Yang Q, Cao J, Xie N, Velletri T, Zhang X, *et al*: Fate decision of mesenchymal stem cells: Adipocytes or osteoblasts? Cell Death Differ 23: 1128-1139, 2016.
5. Tae JY, Lee H, Lee H, Ko Y and Park JB: Osteogenic potential of cell spheroids composed of varying ratios of gingiva-derived and bone marrow stem cells using concave microwells. Exp Ther Med 16: 2287-2294, 2018.
6. Almalki SG and Agrawal DK: Key transcription factors in the differentiation of mesenchymal stem cells. Differentiation 92: 41-51, 2016.
7. He S, Yang S, Zhang Y, Li X, Gao D, Zhong Y, Cao L, Ma H, Liu Y, Li G, *et al*: LncRNA ODIR1 inhibits osteogenic differentiation of hUC-MSCs through the FBXO25/H2BK120ub/H3K4me3/OSX axis. Cell Death Dis 10: 947, 2019.
8. Yin Q, Wang J, Fu Q, Gu S and Rui Y: CircRUNX2 through has-miR-203 regulates RUNX2 to prevent osteoporosis. J Cell Mol Med 22: 6112-6121, 2018.
9. Li CJ, Cheng P, Liang MK, Chen YS, Lu Q, Wang JY, Xia ZY, Zhou HD, Cao X, Xie H, *et al*: MicroRNA-188 regulates age-related switch between osteoblast and adipocyte differentiation. J Clin Invest 125: 1509-1522, 2015.
10. Moerman EJ, Teng K, Lipschitz DA and Lecka-Czernik B: Aging activates adipogenic and suppresses osteogenic programs in mesenchymal marrow stroma/stem cells: The role of PPAR-gamma2 transcription factor and TGF-beta/BMP signaling pathways. Aging Cell 3: 379-389, 2004.
11. Wu J, Zhang W, Ran Q, Xiang Y, Zhong JF, Li SC and Li Z: The differentiation balance of bone marrow mesenchymal stem cells is crucial to hematopoiesis. Stem Cells Int 2018: 1540148, 2018.
12. Yu B and Wang CY: Osteoporosis: The result of an 'aged' bone microenvironment. Trends Mol Med 22: 641-644, 2016.
13. Khosla S and Hofbauer LC: Osteoporosis treatment: Recent developments and ongoing challenges. Lancet Diabetes Endocrinol 5: 898-907, 2017.
14. Cheung CL, Xiao SM and Kung AW: Genetic epidemiology of age-related osteoporosis and its clinical applications. Nat Rev Rheumatol 6: 507-517, 2010.
15. Carey JJ, Lewiecki EM, Blank RD, Shuhart CR and Buehring B: Treatment of low bone density or osteoporosis to prevent fractures in men and women. Ann Intern Med 167: 901, 2017.
16. Lorentzon M and Cummings SR: Osteoporosis: The evolution of a diagnosis. J Intern Med 277: 650-661, 2015.
17. Sànchez-Riera L, Carnahan E, Vos T, Veerman L, Norman R, Lim SS, Hoy D, Smith E, Wilson N, Nolla JM, *et al*: The global burden attributable to low bone mineral density. Ann Rheum Dis 73: 1635-1645, 2014.
18. Turpeinen H, Ortutay Z and Pesu M: Genetics of the first seven proprotein convertase enzymes in health and disease. Curr Genomics 14: 453-467, 2013.
19. Osathanon T, Manokawinchoke J, Sa-Ard-Iam N, Mahanonda R, Pavasant P and Suwanwela J: Jagged1 promotes mineralization in human bone-derived cells. Arch Oral Biol 99: 134-140, 2019.
20. McPherron AC, Lawler AM and Lee SJ: Regulation of anterior/posterior patterning of the axial skeleton by growth/differentiation factor 11. Nat Genet 22: 260-264, 1999.
21. Liu H, Sun Q, Wan C, Li L, Zhang L and Chen Z: MicroRNA-338-3p regulates osteogenic differentiation of mouse bone marrow stromal stem cells by targeting Runx2 and Fgfr2. J Cell Physiol 229: 1494-1502, 2014.
22. Zhang XH, Geng GL, Su B, Liang CP, Wang F and Bao JC: MicroRNA-338-3p inhibits glucocorticoid-induced osteoclast formation through RANKL targeting. Genet Mol Res 15: gmr.15037674, 2016.
23. Niu D, Gong Z, Sun X, Yuan J, Zheng T, Wang X, Fan X, Mao Y, Liu X, Tang B, *et al*: miR-338-3p regulates osteoclastogenesis via targeting IKKβ gene. In Vitro Cell Dev Biol Anim 55: 243-251, 2019.
24. Benisch P, Schilling T, Klein-Hitpass L, Frey SP, Seefried L, Raaijmakers N, Krug M, Regensburger M, Zeck S, Schinke T, *et al*: The transcriptional profile of mesenchymal stem cell populations in primary osteoporosis is distinct and shows overexpression of osteogenic inhibitors. PLoS One 7: e45142, 2012.
25. Livak KJ and Schmittgen TD: Analysis of relative gene expression data using real-time quantitative PCR and the 2(-Delta Delta C(T)) Method. Methods 25: 402-408, 2001.

26. Li Y, Zheng F, Xiao X, Xie F, Tao D, Huang C, Liu D, Wang M, Wang L, Zeng F, *et al*: CircHIPK3 sponges miR-558 to suppress heparanase expression in bladder cancer cells. EMBO Rep 18: 1646-1659, 2017.
27. Szumska D, Pieles G, Essalmani R, Bilski M, Mesnard D, Kaur K, Franklyn A, El Omari K, Jefferis J, Bentham J, *et al*: VACTERL/caudal regression/Currarino syndrome-like malformations in mice with mutation in the proprotein convertase Pcsk5. Genes Dev 22: 1465-1477, 2008.
28. Hoac B, Susan-Resiga D, Essalmani R, Marcinkiweicz E, Seidah NG and McKee MD: Osteopontin as a novel substrate for the proprotein convertase 5/6 (PCSK5) in bone. Bone 107: 45-55, 2018.
29. Marie PJ: Targeting integrins to promote bone formation and repair. Nat Rev Endocrinol 9: 288-295, 2013.
30. Eastell R, O'Neill TW, Hofbauer LC, Langdahl B, Reid IR, Gold DT and Cummings SR: Postmenopausal osteoporosis. Nat Rev Dis Primers 2: 16069, 2016.
31. Long H, Sun B, Cheng L, Zhao S, Zhu Y, Zhao R and Zhu J: miR-139-5p represses BMSC osteogenesis via targeting Wnt/β-catenin signaling pathway. DNA Cell Biol 36: 715-724, 2017.
32. Zhang S, Liu Y, Zheng Z, Zeng X, Liu D, Wang C and Ting K: MicroRNA-223 suppresses osteoblast differentiation by inhibiting DHRS3. Cell Physiol Biochem 47: 667-679, 2018.
33. Fu L, Liu H and Lei W: MiR-596 inhibits osteoblastic differentiation and cell proliferation by targeting Smad3 in steroid-induced osteonecrosis of femoral head. J Orthop Surg Res 15: 173, 2020.
34. Zhou S, Qian B, Wang L, Zhang C, Hogan MV and Li H: Altered bone-regulating myokine expression in skeletal muscle Of Duchenne muscular dystrophy mouse models. Muscle Nerve 58: 573-582, 2018.
35. Bartold M, Gronthos S, Haynes D and Ivanovski S: Mesenchymal stem cells and biologic factors leading to bone formation. J Clin Periodontol 46 (Suppl 21): 12-32, 2019.
36. Alcorta-Sevillano N, Macías I, Rodríguez CI and Infante A: Crucial role of Lamin A/C in the migration and differentiation of MSCs in bone. Cells 9: E1330, 2020.